Journal of Power Sources 210 (2012) 374–380

Contents lists available at SciVerse ScienceDirect

Journal of Power Sources

journal homepage: www.elsevier.com/locate/jpowsour

Lanthanum promoted NiO–SDC anode for low temperature solid oxide fuel cells fueled with methane

Aiyu Yan, Monrudee Phongaksorn, Damien Natival, Eric Croiset*

Department of Chemical Engineering, University of Waterloo, 200 University Ave West, Waterloo, Ontario N2L 3G1, Canada

ARTICLE INFO

Article history:
Received 12 September 2011
Received in revised form 21 October 2011
Accepted 22 October 2011
Available online 25 October 2011

Keywords:
Low temperature solid oxide fuel cell
Methane
Lanthanum promotion
NiO–SDC anode

ABSTRACT

A $Ni_{0.95}La_{0.05}O$–SDC composite was tested as solid oxide fuel cell (SOFC) anode fueled with methane at temperatures between 500 and 600 °C (i.e. for low temperature SOFC). It was found that NiO and La_2O_3 formed a solid solution and small amounts of La_2NiO_4 were also observed after sintering at 1340 °C. After subsequent reduction, NiO was reduced to Ni while La_2O_3 remained as oxide phase. The La modified NiO–SDC anode showed higher OCV, over 30% improved maximum power density and better stability in humidified methane fuel as compared with the NiO–SDC anode. Meanwhile, the $Ni_{0.95}La_{0.05}O$–SDC anode cell displayed lower polarization resistance (e.g. at 600 °C, 0.12 Ω cm^{-2} versus 0.34 Ω cm^{-2} for NiO–SDC) implying higher surface reaction activity than the NiO–SDC anode cell. At 600 °C, the $Ni_{0.95}La_{0.05}O$–SDC anode exhibited similar performance and activity in H_2 and CH_4 fuels. The SEM results indicated that La effectively prevented NiO coarsening giving rise to a much finer structure with smaller particle size and more uniform distribution, which can contribute to the better performance with La.

1. Introduction

Solid oxide fuel cells (SOFCs) convert the chemical energy of the fuels directly to electrical energy, offer efficient heat utilization, and low emissions. Intermediate and low temperature (<800 °C) SOFCs have recently received considerable attention due to their expected improved stability, reliability and reduced cost [1,2]. SOFCs' operation at lower temperatures could enable the use of inexpensive metal components as interconnects, improve the stability and durability of all components and provide faster start-up and shutdown procedures. Ceria based electrolyte materials such as SDC and GDC exhibit higher ionic conductivity than the conventional YSZ at reduced temperatures and have been considered as promising electrolyte for intermediate and low temperature SOFCs.

Because of their high operating temperatures (500–1000 °C), SOFCs can internally reform hydrocarbon fuels. In particular, SOFC fueled with methane has attracted considerable attention because natural gas (whose main component is methane) is a widely available fuel and also because it poses lesser challenges than heavier hydrocarbons. One difficulty is that the activation of methane and hydrocarbon requires higher energy than for hydrogen, especially at lower temperatures. In addition, the use of state-of-art Ni-based anode catalysts results in carbon formation (coking), which deactivates and mechanically damages Ni-based SOFCs [3–6]. In order to overcome these drawbacks, considerable efforts have been devoted to develop alternative anode catalysts. For example, Gorte's group [7,8] replaced Ni with Cu which does not catalyze carbon formation; Murray and coworkers [9] used ceria-containing anodes and low operating temperatures to avoid carbon deposition; Zhan and Barnett [10] introduced a Ru–CeO_2 functional layer into the conventional anode and achieved stable power densities in octane fuel; Irvine's group [11,12] developed perovskite-type anodes which were active for methane oxidation at high temperatures. All these strategies showed improved coke-tolerance but suffered from low activity or high cost.

Ni-based anodes are still very attractive candidates for SOFCs if their activity and stability towards methane or hydrocarbon could be improved. Alternative approaches involve addition of alkali, alkali-earth and rare-earth elements such as MgO, CaO, La_2O_3 and Li_2O_3 to Ni-anode [13–16]. It is generally claimed that these additives can prevent Ni coarsening as well as agglomeration resulting in highly dispersed Ni, and lead to stronger basicity which promotes the interaction with the reactants [13–17]. Lanthanum is a well recognized additive for supported catalysts that modifies surface properties of the support and the interface energy between the catalysts and the support [18–20]. It was widely used in reforming and partial oxidation of methane [21–23], and was recently also employed in SOFC anode. Tu et al. [24] modified a Ni–YSZ anode

* Corresponding author. Tel.: +1 519 888 4567x36472; fax: +1 519 746 4979.
E-mail address: ecroiset@uwaterloo.ca (E. Croiset).

0378-7753/$ – see front matter © 2011 Elsevier B.V. All rights reserved.
doi:10.1016/j.jpowsour.2011.10.081

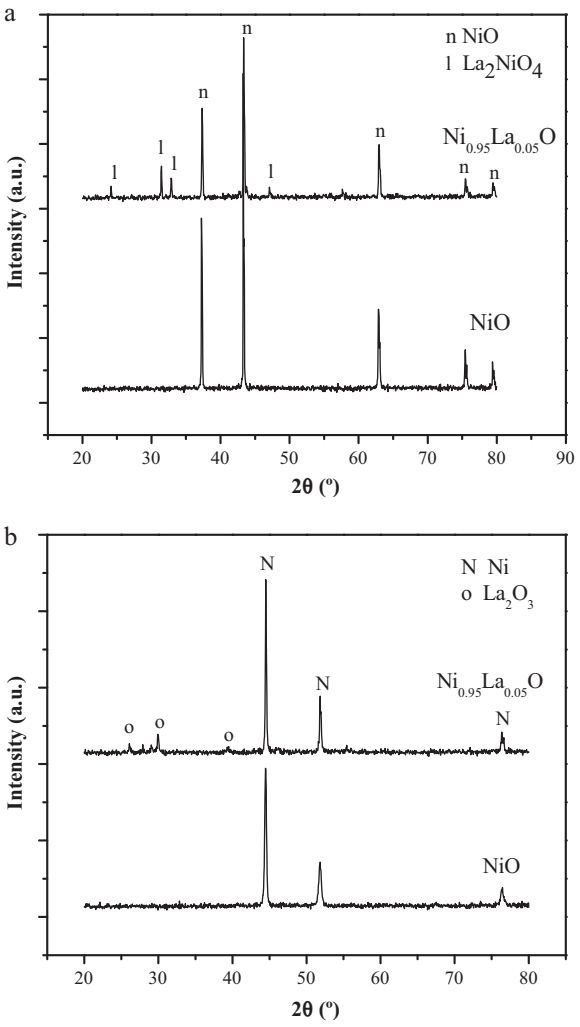

Fig. 1. XRD patterns of NiO and $Ni_{0.95}La_{0.05}O$ powders. (a) Sintered at 1340 °C and (b) after reduction at 700 °C in pure H_2 for 4 h. (n) NiO, (l) La_2NiO_4, (N) Ni, and (o) La_2O_3.

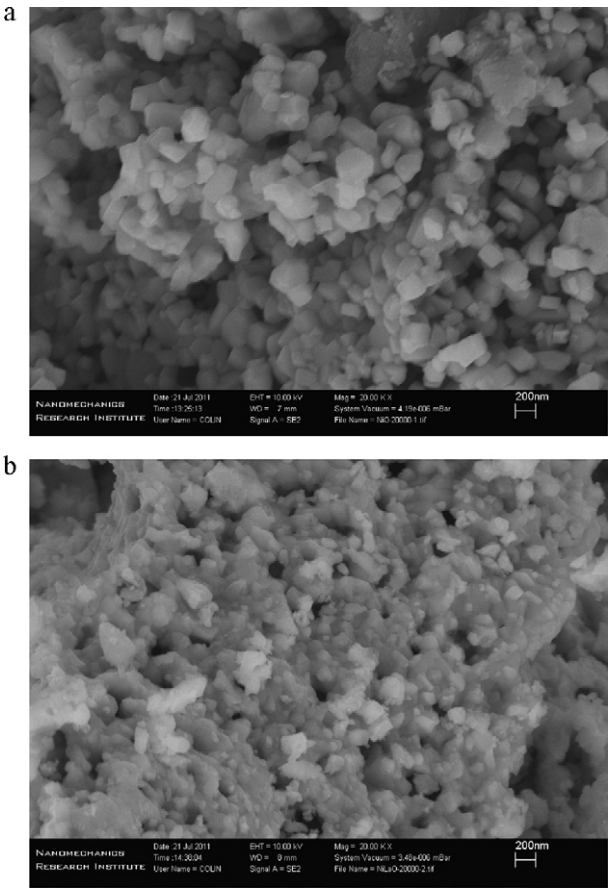

Fig. 2. SEM images of the NiO (a) and $Ni_{0.95}La_{0.05}O$ (b) powders.

with small amounts of La which effectively hindered the sintering of nickel and improved the interfacial contact of NiO and YSZ. Reduced polarization resistance and increased activity for electrochemical oxidation of hydrogen and methane was achieved. Wang et al. [15] used LaNi–Al_2O_3 as a catalyst layer on a Ni–ScSz anode supported cell and found that La greatly reduced carbon deposition under pure methane atmosphere.

However, most of the above mentioned work was done over YSZ or ScSZ based cell with operating temperature above 650 °C. In the present work, we introduced small amount of La into a Ni–SDC cermet for operation at temperatures below 600 °C in order to improve the activity and stability of NiO catalysts towards methane at low SOFC temperatures.

2. Experimental

The NiO, $Ni_{0.95}La_{0.05}O$ and SDC powders were prepared by a glycine–nitrate-process [25]. The proper amount of $M(NO_3)$ (M = Ni, La, Ce, Sm) with desired ratio of glycine were dissolved in D.I. water and heated at 90 °C until a gel was formed. The gel was then heated on an electronic stove igniting to flame. The obtained raw powder was either calcined at 850 °C for 4 h to obtain NiO and $Ni_{0.95}La_{0.05}O$ powder, or at 800 °C for 2 h to obtain SDC powder.

The Ni(La)O–SDC (55:45 wt.%) anode-supported cells were fabricated using a dry-pressing method. The mixture of Ni(La)O and SDC, plus 5 wt% PVB and 5 wt% n-DOP as pore former, was pressed into a pellet with 20 mm diameter to form the anode. The SDC powder was distributed onto the surface of the anode and co-pressed to obtain a green assembly, which was further co-sintered at 1340 °C for 5 h in ambient air. The cathode slurry containing 70 wt% $Sm_{0.5}Sr_{0.5}CoO_3$ (SSC) and 30% SDC was painted onto the SDC film, and fired at 1000 °C for 2 h. The effective area of the cathode was 0.28 cm^2, and the thickness was about 50 μm. The thickness of the electrolyte and anode was 25 and 700 μm, respectively.

The cell performance was tested on an in-house test station. The single cell was in situ reduced in humidified H_2 for several hours at 700 °C and then electrochemically evaluated under potentiodynamic, galvanostatic and impedance modes using a Solartron 1287 potentiostat and a 1260 frequency response analyzer from 600 to 500 °C. The anode was supplied with humidified hydrogen (3% H_2O) at 80 ml min^{-1} or humidified methane (3% H_2O) at 40 ml min^{-1} and the cathode was supplied with air at a flow rate of 100 ml min^{-1}. The gavolnostatic test was performed under a current density of 0.44 A cm^{-2}. The Electrochemical Impedance Spectroscopy (EIS) measurements were carried out under open circuit conditions in the frequency range 0.1 Hz to 5 kHz with a signal amplitude of 10 mV.

In order to determine the crystal structure and phase of NiO and $Ni_{0.95}La_{0.05}O$ after sintering at 1340 °C and after reduction at 700 °C in hydrogen for 4 h, XRD was conducted on a Bruker D8 FOCUS diffractometer using Cu Kα radiation (λ = 1.5425 Å) in 2θ ranging from 20° to 80°. The microstructure and elemental composition of the anode before and after operation in methane were analyzed by SEM and EDX (LEO 1530).

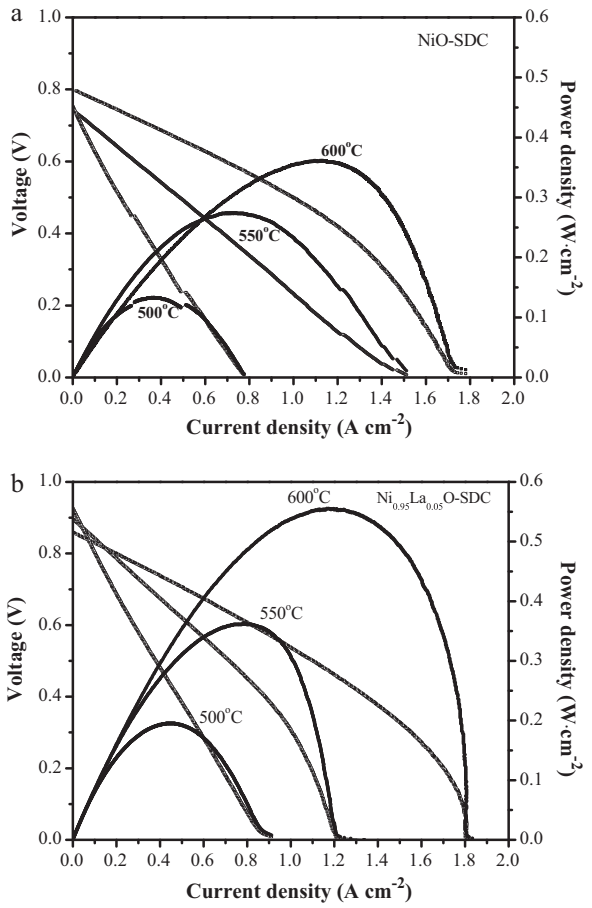

Fig. 3. *I–V* and *I–P* curves of the cells in 3% H_2O humidified methane fuel from 500 to 600 °C. (a) NiO–SDC anode cell and (b) $Ni_{0.95}La_{0.05}O$–SDC anode cell.

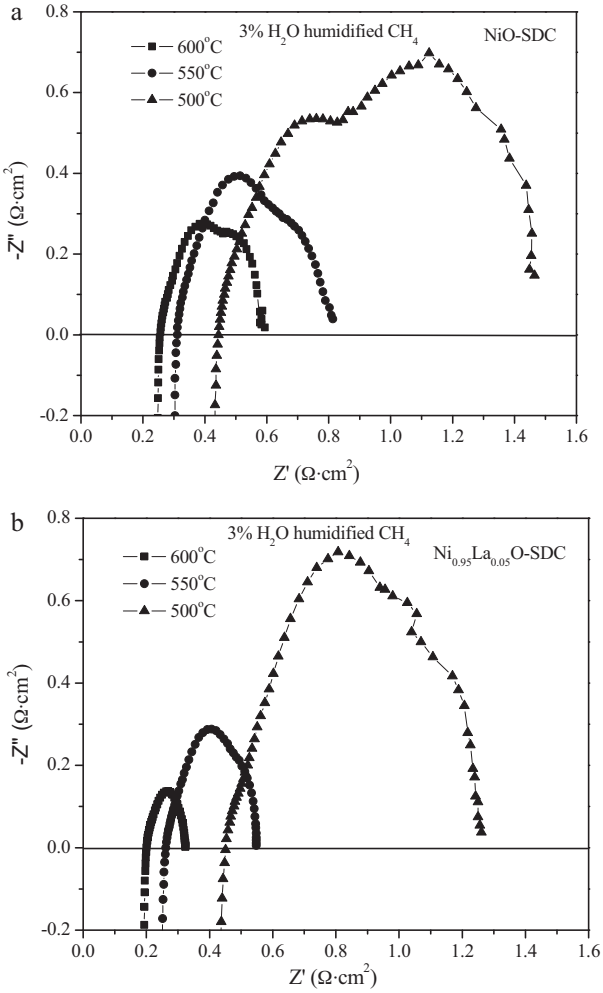

Fig. 4. Electrochemical impedance spectra of the cells in 3% H_2O humidified CH_4 from 500 to 600 °C. (a) NiO–SDC anode cell and (b) $Ni_{0.95}La_{0.05}O$–SDC anode cell.

3. Results and discussion

3.1. Property of the powder

Fig. 1(a) gives the XRD patterns of the NiO and $Ni_{0.95}La_{0.05}O$ powders after sintering at 1340 °C. Typical diffractions from the NiO phase at 37.2°, 43.2°, 62.6°, 75.3° and 79.2° [26] were observed from the XRD patterns of both materials. Reflection peaks at 24.2°, 31.3°, 32.8° and 47.1°, which could be assigned to La_2NiO_4 [27], also appeared on the XRD pattern of $Ni_{0.95}La_{0.05}O$, suggesting that a small amount of NiO and La_2O_3 reacted with each other giving rise to the formation of a secondary phase. It was reported that La_2NiO_4 exhibited good electrical and ionic conductivities [28]. Therefore, small amounts of La_2NiO_4 should not be harmful to the anode.

In real operating conditions, the NiO was first reduced to Ni which acts as the electrochemical catalyst and electronic conductor. Therefore, the NiO and $Ni_{0.95}La_{0.05}O$ powders were reduced in pure H_2 for 4 h at 700 °C and the obtained powders were characterized by XRD. As can be seen in Fig. 1(b), strong diffraction peaks from Ni appeared on the XRD patterns of both samples [29]. La_2O_3 was not reduced and remained as oxide phase [30]. The peak from La_2NiO_4 disappeared since it could also be reduced to Ni and La_2O_3 [27], further confirming that it was not harmful to the cell.

Shown in Fig. 2 are the SEM images of the as prepared NiO and $Ni_{0.95}La_{0.05}O$ powders. The primary grains of $Ni_{0.95}La_{0.05}O$ were in the range 20 to 100 nm. As for NiO, jagged crystallized particles in the size of 150–400 nm were observed. Both materials aggregated into bigger particles in micron size.

3.2. Electrochemical test of the cells

Fig. 3(a) and (b) presents the *I–V* and *I–P* curves of the cells with NiO–SDC anode and $Ni_{0.95}La_{0.05}O$–SDC anode, respectively, operating with 3% H_2O humidified CH_4 between 500 and 600 °C. For the NiO–SDC cell, peak power densities as high as 0.36, 0.27 and 0.13 W cm^{-2} were obtained at 600, 550 and 500 °C, respectively. The power densities of the SDC thin film SOFC in methane reported by different groups varied greatly, ranging from ~0.1 to ~1 W·cm^{-2} at 600 °C [31–34]. The performance of the cells is influenced by various factors such as the thickness of the layers, anode composition, as well as cathode and the fuel compositions. Thinner electrolyte film (e.g. <25 μm) and more active cathode (e.g. $Ba_{0.5}Sr_{0.5}Co_{0.8}Fe_{0.2}O_{3-\delta}$) could lead to higher performance [35]. In addition, the microstructure of the cell plays an important role in the performance, which will be discussed later. It can be seen from Fig. 3(a) that the OCV of the cell was lower than the theoretical electromotive force. For instance, the OCV at 600 °C was 0.80 V while the theoretical one is 1.13 V. It is well known that the doped ceria electrolyte exhibits mixed ionic and electronic conduction under reducing atmosphere, which originates from the partial reduction of Ce^{4+} into Ce^{3+}. Therefore, the open circuit voltage of the fuel cell with doped ceria electrolyte is usually lower than the theoretical value due to the inner efficiency loss.

With 5 mol% La doping into NiO, the peak power densities of the cell were significantly increased. The respective maximum power

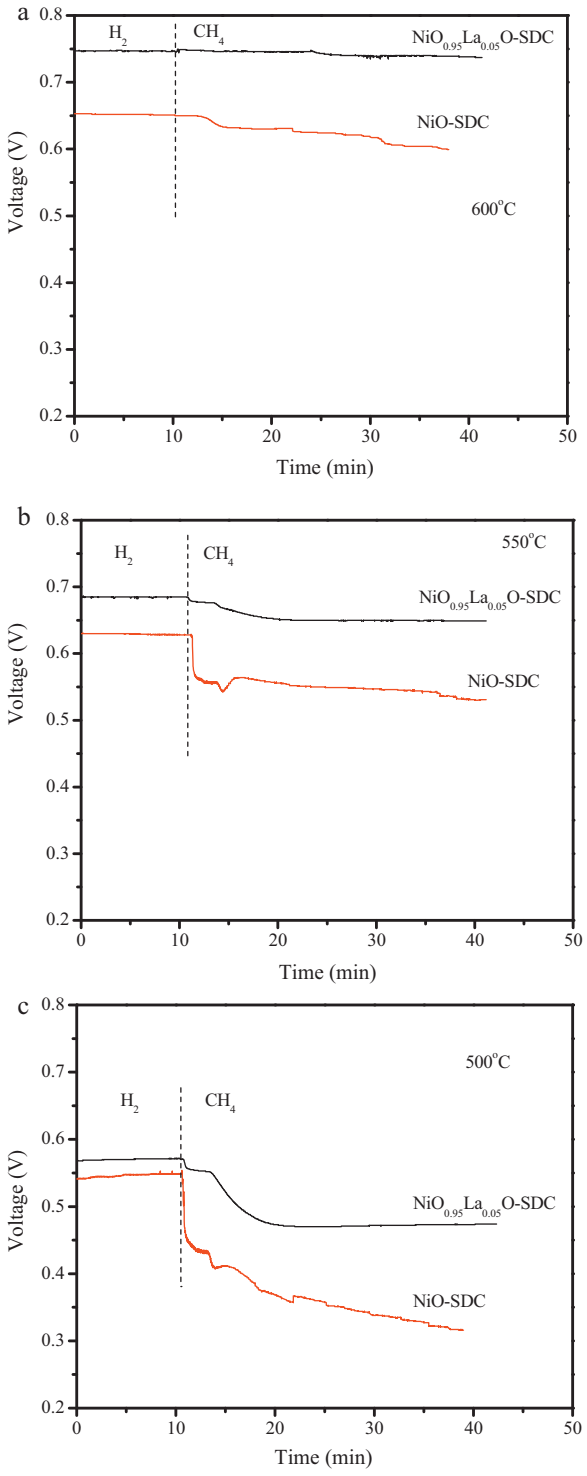

Fig. 5. Voltage of the cells versus time at a constant current density of 0.44 A cm^{-2} at various temperatures. (a) 600 °C, (b) 550 °C, and (c) 500 °C.

densities at 600, 550 and 500 °C were 0.55, 0.36 and 0.20 W cm^{-2}, which corresponded to a 53%, 33% and 54% improvement as compared with the NiO–SDC anode cell. Comparison between Fig. 3a and b indicates that the OCV of the $Ni_{0.95}La_{0.05}O$–SDC anode cell was also higher than with the NiO–SDC anode cell. For example, the OCV of the former was 0.87 V at 600 °C while that of the latter was 0.80 V. It has been reported that the electrode activity also affected the OCV of SOFC [35,36]. A similar improvement phenomenon was observed by McIntosh et al. [37] when they doped precious

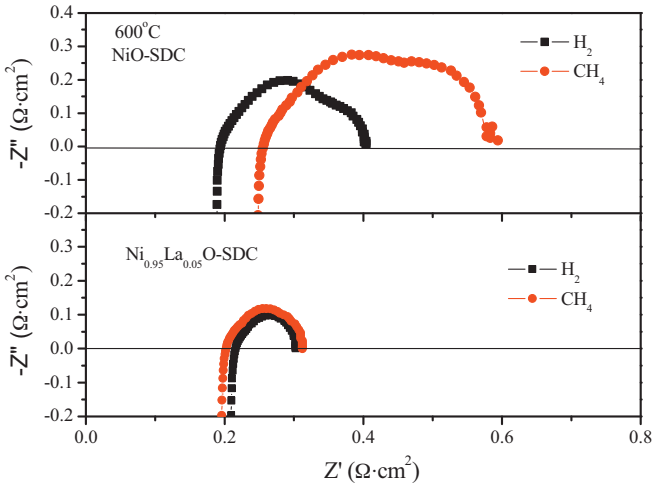

Fig. 6. Comparison of the electrochemical impedance spectra of different cells in 3% H_2O humidified H_2 and CH_4 fuels at 600 °C.

metals into SOFC anodes. They considered the difference between the measured OCV and the Nernst potentials as representing an energy loss due to surface reaction limitations. The addition of a better oxidation catalyst in the anode lowered this loss remarkably, which could explain the reason of the enhanced OCV.

In Fig. 4, the electrochemical impedance spectra of the cells with different anodes are presented. The polarization resistances (R_p) of each cell at different temperatures were derived from the spectra and are listed in Table 1. The impedances of the cells were measured by using a two electrode configuration. Thus, the obtained impedance was the combination of the anode, cathode and electrolyte. Since the cathode and electrolyte were identical for all cells, differences in the impedance spectra could be assigned only to differences in the anode at a given temperature. Obviously, the $Ni_{0.95}La_{0.05}O$–SDC anode cell showed much lower R_p than the NiO–SDC anode cell. For example, R_p of

Table 1
Polarization resistance of NiO–SDC and $Ni_{0.95}La_{0.05}O$–SDC anode cells in methane from 500 to 600 °C.

	600 °C	550 °C	500 °C
R_p (Ω cm^2) NiO–SDC	0.34	0.50	0.86
R_p (Ω cm^2) $Ni_{0.95}La_{0.05}O$–SDC	0.12	0.29	0.51

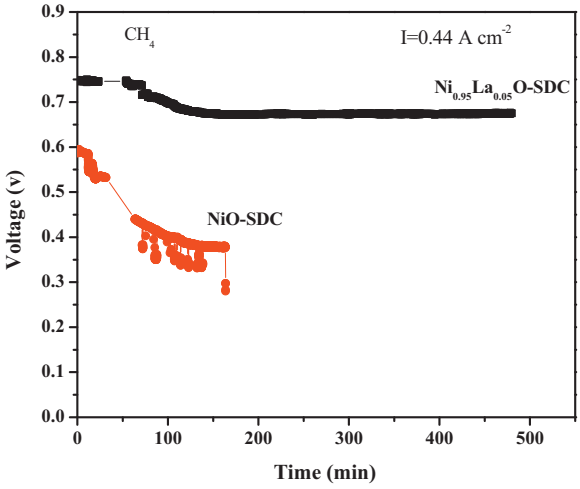

Fig. 7. Stability of the cells operated in 3% H_2O humidified CH_4 at a constant current density of 0.44 A cm^{-2} at 600 °C.

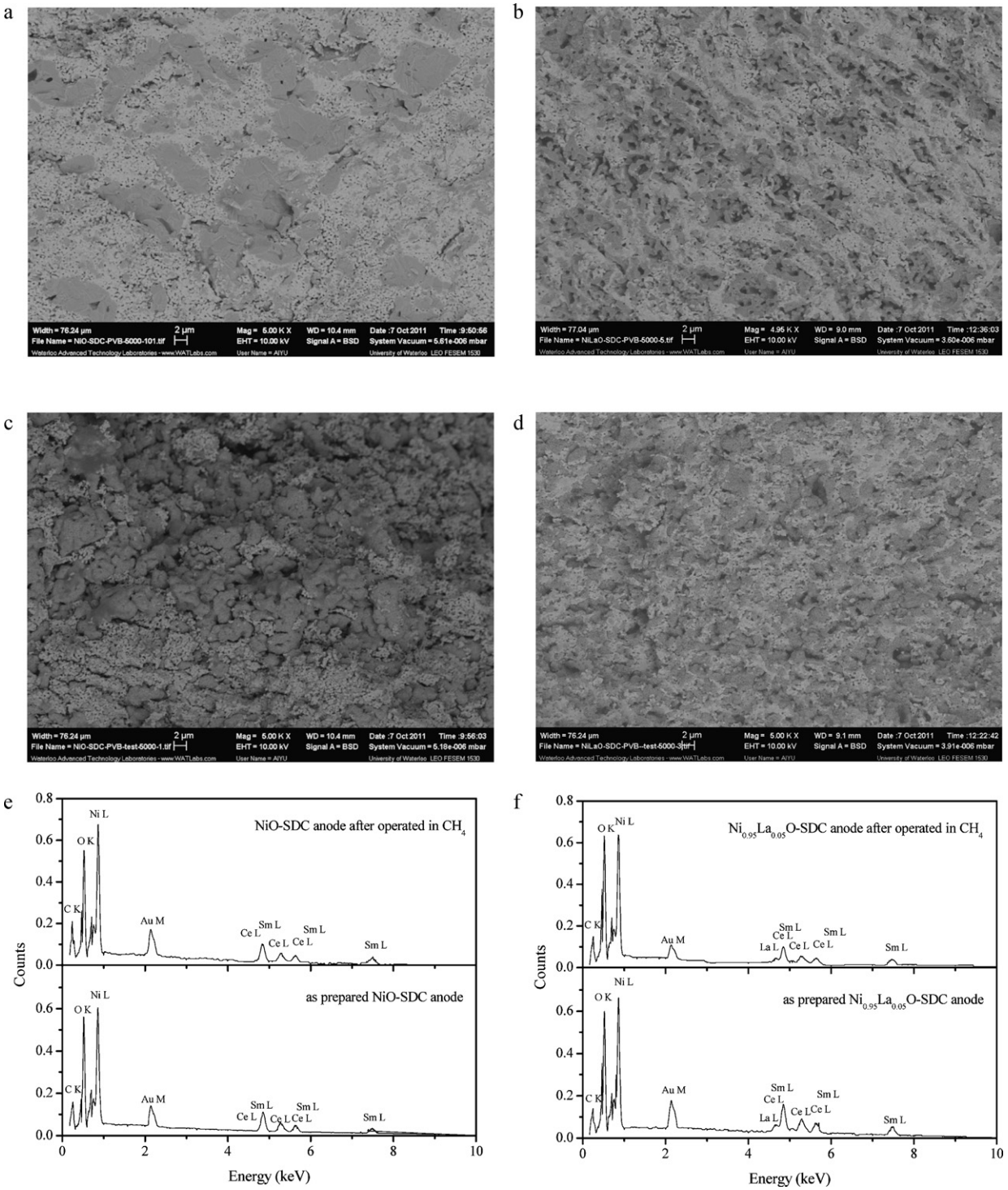

Fig. 8. SEM images and EDX spectra of the anode of different cells from cross section. (a) as prepared NiO–SDC anode (b) as prepared $Ni_{0.95}La_{0.05}O$–SDC anode (c) NiO–SDC anode after operated in 3% H_2O humidified CH_4 for 160 min (d) $Ni_{0.95}La_{0.05}O$–SDC anode after operated in 3% H_2O humidified CH_4 for 480 min (e) comparison of EDX spectra of NiO–SDC anode before and after operated in 3% H_2O humidified CH_4 (f) comparison of EDX spectra of $Ni_{0.95}La_{0.05}O$–SDC anode before and after operated in 3% H_2O humidified CH_4.

$Ni_{0.95}La_{0.05}O$–SDC anode cell was 0.12 $\Omega\,cm^{-2}$ at 600 °C while that of NiO–SDC anode cell was 0.34 $\Omega\,cm^2$. The former was less than half the value of the latter. The polarization resistance originates from the electrochemical processes occurring at the electrode. Therefore, the lower R_p suggests faster reaction kinetic over the electrode. It has been widely recognized that La_2O_3 could act as a promoter and improve the catalytic activity of Ni towards methane reforming. Cui et al. [22] reported that proper amount of La_2O_3 resulted in smaller size of Ni particles and more Ni active sites which facilitated CO_2 reforming of methane. Zhang and Verykios [23] proposed that the interaction between Ni crystallites and La_2O_3 support or La species which were decorating the Ni crystallites led to unusual chemisorptive and catalytic behavior of Ni/La_2O_3 catalyst. Wang et al. [16] investigated the La_2O_3 promoted Ni–Al_2O_3 as catalyst layer for a ScSZ-based SOFC operating on methane and suggested that the introduction of La_2O_3

could prevent the alumina support from thermal deterioration and increase the basicity of the catalyst, giving rise to enhanced catalytic activity and coke tolerance. From the XRD results given in Fig. 1, it can be seen that NiO and La_2O_3 have strong interactions and exist as solid solution and La_2NiO_4 states. After reduction, NiO was reduced to Ni and La_2O_3 remained as oxide state. It was possible that La_2O_3 modified the surface property of Ni and enhanced its activity towards methane. Additionally, La_2O_3 also could modify the particles morphologically as proved in Fig. 2. The improved microstructure was another reason contributing to the decreased polarization resistance, which will be discussed later.

The higher reaction activity of $Ni_{0.95}La_{0.05}O$–SDC anode over NiO–SDC anode was further proven when comparing their performance in humidified CH_4 and humidified H_2. Fig. 5 shows the change in voltage at a constant current density of 0.44 A cm^{-2} as the fuel was switched from H_2 to CH_4 for temperatures of 500, 550 and 600 °C. At 600 °C, the voltage of the NiO–SDC anode cell was 0.65 V with humidified H_2 and then gradually reduced to 0.60 V after being fed with humidified CH_4 for 30 min. On the other hand, the $Ni_{0.95}La_{0.05}O$–SDC anode cell displayed almost the same voltage of 0.74 V in H_2 and CH_4, indicating that $Ni_{0.95}La_{0.05}O$ showed similar activity towards H_2 and CH_4 under the investigated conditions. This result was in line with the information deduced from the impedance spectra measured at 600 °C. As can be seen in Fig. 6, the polarization resistance of NiO–SDC anode cell increased from 0.21 to 0.34 Ω cm^2 when the fuel was switched from H_2 to CH_4. In contrast, the impedance spectra of $Ni_{0.95}La_{0.05}O$–SDC anode cell in H_2 and CH_4 nearly overlapped. At 550 and 500 °C, $Ni_{0.95}La_{0.05}O$–SDC anode cell had lower performance in CH_4 than in H_2. The voltage decreased from 0.68 to 0.65 V at 550 °C and from 0.57 to 0.47 V at 500 °C in 10 min and then reached a steady state. It can be inferred that the $Ni_{0.95}La_{0.05}O$–SDC anode exhibited superior activity towards methane at higher temperature. As for the NiO–SDC anode, the voltage decreased from 0.63 to 0.53 V and from 0.54 to 0.32 V at 550 and 500 °C in 30 min, respectively. Obviously, the reduction of the performance over NiO–SDC was much serious than that over $Ni_{0.95}La_{0.05}O$–SDC.

After the tests mentioned above were completed, the cells were heated to 600 °C again and operated under galvanostatic mode with 0.44 A cm^{-2} in 3% H_2O humidified methane. As shown in Fig. 7, the voltage for the NiO–SDC anode cell dropped continually from 0.59 V to 0.38 V during 160 min. There were also fluctuations of the voltage in the process, which might result from cracks of the cell and subsequent direct combustion of CH_4. However, the $Ni_{0.95}La_{0.05}O$–SDC anode cell remained stable over 480 min. The cell showed the same voltage as the initial value of 0.74 V and kept this value during the first 60 min, followed by decreasing slowly to 0.67 V and finally stabilizing at this value until termination of the experiment after 480 min.

3.3. Microstructure of the cells

The SEM images of the as prepared and spent anodes after operation in 3% H_2O humidified CH_4 (Fig. 8) provide some direct information on the micro-structural difference between the $Ni_{0.95}La_{0.05}O$–SDC anode and the NiO–SDC anode. For the NiO–SDC anode, the NiO showed quite coarse structure and serious agglomeration. The particle size of NiO was ranging from 2 to 20 μm. On the other hand, the $Ni_{0.95}La_{0.05}O$–SDC anode exhibited much finer structure with smaller particle size, more uniform distribution, higher porosity and better connection between particles. It is well known that the microstructure of the cell played an important role in the electrochemical reaction taking place on the electrode. For example, the apparent activation energy of the polarization resistance was high when nickel and YSZ were the point contacts or if the Ni–YSZ cermets were coarse, while it was low if the anodes had a fine structure [38,39]. The fine microstructure led to an increase in the electrode porosity and triple phase boundary (TPB) length, which not only improved the transport of gas reactant but also enlarged the reaction zone. Therefore, the modified microstructure of the $Ni_{0.95}La_{0.05}O$–SDC anode was one of the key reasons for the higher performance and lower polarization resistance. After operation in humidified CH_4, the NiO–SDC anode showed poor connections between particles and even cracks on the cell. The Ni particles in the $Ni_{0.95}La_{0.05}O$–SDC anode became a little coarser than the as prepared cell too, but still kept intact shape.

Energy-dispersive X-ray (EDX) was used to analyze the elemental compositions of the anodes before and after operation in 3% H_2O humidified CH_4. The corresponding spectra are given in Fig. 8e and f. For the as prepared NiO–SDC anode, the content of carbon, which originated from contamination or from the organic pore former, was 3.02 wt%. After operation in 3% H_2O humidified CH_4, the C signal was intensified and its content increased to 5.58 wt%, implying that coking occurred. On the other hand, for $Ni_{0.95}La_{0.05}O$–SDC anode cell, the C content only slightly increased from 2.56 wt% to 3.10 wt% after operation in humidified CH_4. It can be deduced that $Ni_{0.95}La_{0.05}O$–SDC anode exhibited higher coke resistance than NiO–SDC anode.

4. Conclusions

It was demonstrated that the addition of 5 mol% La into NiO–SDC anode could effectively improve the OCV, performance and stability of the cell when operating on methane at temperatures between 500 and 600 °C. La modification of the nickel catalyst reduced the polarization resistance and increased the activity for methane. Particularly, the $Ni_{0.95}La_{0.05}O$–SDC anode exhibited similar performance and activity in humidified H_2 and CH_4 fuel at 600 °C. It was found that the $Ni_{0.95}La_{0.05}O$–SDC anode cell showed finer structure with smaller particle size and more uniform distribution than the NiO–SDC anode cell, which played an important role in the improved performance.

Acknowledgements

This research was supported through funding to the NSERC Solid Oxide Fuel Cell Canada Strategic Research Network from the Natural Science and Engineering Research Council (NSERC) and other sponsors listed at www.sofccanada.com.

References

[1] M. Shiono, K. Kobayashi, T.L. Nguyen, K. Hosoda, T. Kato, K. Ota, M. Dokiya, Solid State Ionics 170 (2004) 1–7.
[2] B. Zhu, X.T. Yang, J. Xu, Z.G. Zhu, S.J. Ji, M.T. Sun, J.C. Sun, J. Power Sources 118 (2003) 47–53.
[3] N.Q. Minh, J. Am. Ceram. Soc. 76 (1993) 563–588.
[4] R.M. Ormerod, Chem. Soc. Rev. 32 (2003) 17–28.
[5] R.J. Gorte, S. Park, J.M. Vohs, C.H. Wang, Adv. Mater. 12 (2000) 1465–1469.
[6] M. Mogensen, K. Kammer, Annu. Rev. Mater. Res. 33 (2003) 321–331.
[7] S. Park, J.M. Vohs, R.J. Gorte, Nature 404 (2000) 265–267.
[8] S. McIntosh, R.J. Gorte, Chem. Rev. 104 (2004) 4845–4865.
[9] E.P. Murray, T. Tasai, S.A. Barnett, Nature 400 (1999) 649–651.
[10] Z. Zhan, S.A. Barnett, Science 308 (2005) 844–847.
[11] J.C. Ruiz-Morales, J. Canales-Vázquez, C. Savaniu, D. Marrero-López, W. Zhou, J.T.S. Irvine, Nature 439 (2006) 568–571.
[12] S. Tao, J.T.S. Irvine, Nat. Mater. 2 (2003) 320–323.
[13] Y. Shiratori, Y. Teraoka, K. Sasaki, Solid State Ionics 177 (2006) 1371–1380.
[14] M. Phongaksorn, A. Yan, M. Ismail, A. Ideris, E. Croiset, S. Corbin, Y. Yoo, ECS Trans. 35 (2011) 1683–1688.
[15] W. Wang, R. Ran, Z. Shao, J. Power Sources 196 (2011) 90–97.
[16] W. Wang, C. Su, R. Ran, Z. Shao, J. Power Sources 196 (2011) 3855–3862.
[17] K. Tomishige, Y.-G. Chen, K. Fujimoto, J. Catal. 181 (1999) 91–103.
[18] J.S. Church, N.W. Cant, D.L. Trimm, Appl. Catal. A 101 (1993) 105–116.
[19] H. Schaper, E.B.M. Doesburg, P.H.M. De Korte, L.L. Van Reijen, Solid State Ionics 16 (1985) 261–265.
[20] F. Oudet, A. Vejux, P. Courtine, Appl. Catal. 50 (1989) 79–86.

[21] J. Requies, M.A. Cabrero, V.L. Barrio, M.B. Güemez, J.F. Cambra, P.L. Arias, F.J. Pérez-Alonso, M. Ojeda, M.A. Peña, J.L.G. Fierro, Appl. Catal. A 289 (2005) 214–223.
[22] Y. Cui, H. Zhang, H. Xu, W. Li, Appl. Catal. A 331 (2007) 60–69.
[23] Z. Zhang, X.E. Verykios, Appl. Catal. A 138 (1996) 109–133.
[24] B. Tu, Y. Dong, B. Liu, M. Cheng, J. Power Sources 165 (2007) 120–124.
[25] L.A. Chick, L.R. Pederson, G.D. Maupin, J.L. Bates, L.E. Thomas, G.J. Exarhos, Mater. Lett. 10 (1990) 6–12.
[26] G. Li, X. Huang, Y. Shi, J. Guo, Mater. Lett. 51 (2001) 325–330.
[27] F. Hou, Y. Qin, T. Xu, M. Xu, J. Electroceram. 8 (2002) 243–247.
[28] A. Aguadero, J.A. Alonso, M.J. Martínez-Lope, M.T. Fernández-Díaz, M.J. Escudero, L. Daza, J. Mater. Chem. 16 (2006) 3402–3408.
[29] S. Kumar, S. Kumar, S.K. Chakarvarti, J. Mater. Chem. 39 (2004) 3249–3251.
[30] C. Hu, H. Liu, W. Dong, Y. Zhang, G. Bao, C. Lao, Z.L. Wang, Adv. Mater. 19 (2007) 470–474.
[31] C. Jin, C. Yang, F. Zhao, A. Coffin, F. Chen, Electrochem. Commun. 12 (2010) 1450–1452.
[32] Z. Wang, W. Weng, K. Cheng, P. Du, G. Shen, G. Han, J. Power Sources 179 (2008) 541–546.
[33] A.C. Tavares, B.L. Kuzin, S.M. Beresnev, N.M. Bogdanovich, E.Kh. Kurumchin, Y.A. Dubitsky, A. Zaopo, J. Power Sources 183 (2008) 20–25.
[34] Z. Shao, C. Zhang, W. Wang, C. Su, W. Zhou, Z. Zhu, H.J. Park, C. Kwak, Angew. Chem. 123 (2011) 1832–1837.
[35] T. Matsui, T. Kosaka, M. Inaba, A. Mineshige, Z. Ogumi, Solid State Ionics 176 (2005) 663–668.
[36] A. Yan, M. Cheng, Y. Dong, W. Yang, V. Maragou, S. Song, P. Tsiakaras, Appl. Catal. B 66 (2006) 64–71.
[37] S. McIntosh, J.M. Vohs, R.J. Gorte, Electrochem. Solid State Lett. 6 (2003) A240–A243.
[38] M. Mogensen, S. Skaarup, Solid State Ionics 86–88 (1996) 1151–1160.
[39] M. Brown, S. Primdahl, M. Mogenson, J. Electrochem. Soc. 147 (2000) 475–485.